ELSEVIER

Journal of Volcanology and Geothermal Research 98 (2000) 173–188

Journal of volcanology and geothermal research

www.elsevier.nl/locate/jvolgeores

Geophysical exploration for geothermal low enthalpy resources in Lipari Island, Italy

P.P.G. Bruno[a,*], V. Paoletti[b], M. Grimaldi[b], A. Rapolla[b]

[a]*Osservatorio Vesuviano-Centro di Sorveglianza, Via Diocleziano, 328, 80124 Naples,Italy*
[b]*Dipartimento di Geofisica e Vulcanologia, Università di Napoli Federico II, Largo S. Marcellino, 10, 80138 Naples,Italy*

Received 22 June 1999; received in revised form 15 November 1999; accepted 15 November 1999

Abstract

Integrated geophysical surveys were performed in two sites, Fossa di Fuardo and Terme di San Calogero in Lipari Island, Southern Italy with the intent of the exploration of low-enthalpy geothermal fluids. Both sites show strong geochemical and geologic evidences of hydrothermal activity. The geophysical methods consist of two microgravimetric surveys, two 2D geoelectric profiles, a seismic reflection profile and a five seismic refraction profiles. The seismic methods allowed us to locate the main subsurface seismic discontinuities and to evaluate their geometrical relationships. The gravity field was used to constraint the seismic discontinuities, while the electric prospecting let discriminate more conductive areas, which could correspond to an increase in thermal fluid circulation in the investigated sites.

The results obtained by the different geophysical methods are in good agreement and permit the definition of a reliable geostructural model of the subsurface setting of the two investigated areas. A low-enthalpy geothermal reservoir constituted by a permeable pyroclastic and lava sequence underlying two shallow impermeable formations was found at Fossa del Fuardo. The reservoir is intersected by some sub-vertical faults/fractures that probably play an important role in convoying the thermal water up to the surface. At the other site, Terme di S. Calogero, the geophysical surveys showed that an intense circulation of fluids affects the subsurface of the area. This circulation concentrates along a ENE-trending fault located at a little distance from the thermal resort. The hot fluids may upraise along the fault if the width of the ascent area is smaller than 20 m.

Keywords: Aeolian island; Lipari; geoelectric; seismic reflection; seismic refraction; gravimetry; low enthalpy geothermal exploration

1. Introduction

Lipari is the largest of seven islands constituting the Aeolian archipelago, located in the south-eastern margin of the Tyrrhenian sea (Fig. 1) and interpreted as a volcanic arc sitting about 250 km above the Tyrrhenian Benioff zone (Anderson and Jackson, 1987). The genesis of this area is strictly connected to the ensuing fragmentation, dispersion and subsidence of a formerly continuous lithospheric segment during Miocene to Pliocene. These have led to the formation of the western Mediterranean and the Tyrrhenian basins (Alvarez et al., 1974; Alvarez, 1976; Biji-Duval et al., 1987).

The peri-Tyrrhenian margin of Italy is the site of present-day volcanism. On the northeastern border the recent activities occur on mainland Italy and adjacent islands. On the southeastern border, the volcanic

* Corresponding author. Tel.: + 39-81-6108-437; fax: + 39-81-6100-811.

E-mail address: piebruno@cds.unina.it (P.P.G. Bruno).

0377-0273/00/$ - see front matter
PII: S0377-0273(99)00183-3

activity is concentrated on the Aeolian Arc where there are three still active sub aerial volcanoes: Stromboli, with persistent activity; Vulcano, which had numerous explosive eruptions during historic times, the last of which occurred in 1888–1890; and Lipari where the last eruption took place about 1400 y.b.p in the northeastern part of the island (Keller, 1970). Low-temperature fumaroles (80–90°C) and hot springs are the only present manifestations of volcanic heat in Lipari.

The volcanic and structural evolution of Lipari is well known and only its main features are reported here (Locardi and Nappi, 1979; Pichler, 1980; De Rosa and Sheridan, 1983; Cortese et al., 1986; Gillot, 1987; Crisci et al., 1991; Esperanca et al., 1992). The oldest Lipari products consist of 223–150-kyr-old basalt-andesitic lavas erupted from submarine vents and from subaerial volcanoes. The successive volcanism (from 127 to 92 kyr) occurred in the central sector of the island, where the activity of the Mt. S. Angelo and Costa d'Agosto volcanoes (high-K andesitic lavas and pyroclastics) developed within the Mt. S. Angelo depression. After a gap in volcanic activity of about 50 kyr, volcanism resumed in the southern sector of the island with the emplacement of rhyolitic–shoshonitic pyroclastics and of the N–S-aligned South Lipari and Mt. Guardia domes (42–20 kyr). This activity developed within a pre-existing volcanotectonic depression formed between 92 and 42 kyr. The last phase of activity on Lipari developed in the northeastern sector of the island where the 11.4–1.41-kyr-old N–S-aligned Gabellotto, Forgia Vecchia, and Pilato rhyolitic eruptive centers occur (Fig. 1).

The structural association of Lipari is defined by fault segments and associated fractures which can be grouped in two main sets striking NNW–SSE/NW–SE and from N–S to ENE–WSW (Frazzetta et al., 1982; Ventura, 1994, 1995; Tortorici et al., 1995; Lanzafame and Bousquet, 1997). The NW–SE/NNW–SSE-striking oblique- to strike-slip faults represent the main shear zone whereas the ENE–WSW- and N–S-striking faults represent horsetails and tension fractures, respectively. The N–S faults play an important role in the control of the volcanic activity: the Lipari eruptive centers younger than 42 kyr form a N–S-striking volcanic belt. The NW–SE/NNW–SSE and N–S faults move in response to a regional normal-strike slip stress regime characterized by a subhorizontal s3 axis striking N98°E + 8° (Ventura, 1994; Tortorici et al., 1995). According to Barberi et al. (1994), Ventura (1994) and Lanzafame and Bousquet (1997), the Lipari branch of the "Tindari–Letojanni" fault system forms a composite pull-apart type structure. The volcanotectonic faults bounding the main Lipari depressions follow the same strike of the tectonic structures. Further, the Mt. Guardia depression formed during the longest periods of quiescence in the volcanic activity. These observations suggest the lack of a direct relationship between the formation of volcanotectonic depressions and volcanic processes (i.e. caldera collapses).

The results of previous geological, mesostructural and geochemical prospecting performed in the study area suggest the possible presence of a high-enthalpy geothermal system on the Island. This system, similar to what was observed in analogous geological environments, is probably made up by a magmatic heat source and by a convective circulation of shallow waters that seep through the volcanic rocks. Consequently, these waters are heated by the source and rise back to the earth surface. All thermal emergencies discovered on the island seem connected with the NE and ENE tectonic structures cutting the western sector of Lipari. Along some of these structures, remarkable hydrothermal alteration phenomena that generated kaolin and alum deposits, which are known since ancient times, are present. In the present paper we discuss the results of an integrated geophysical prospecting that was executed in two sites of the island where the highest evidences of this thermal activity are present: "Fossa del Fuardo" and "Terme di San Calogero". In the first site the surveys were carried out over a large hydrothermal alteration area (Fig. 2a). In the second site the prospecting was carried next to the thermal baths (Fig. 3a), which were renewed during the Hellenistic and the Roman times. Unfortunately, due to recent renovation works executed near the thermal baths, the spring was partly drained.

The aim of the surveys was to evaluate in the subsoil of both sites the presence of shallow low-enthalpy thermal fluids (with temperature lower than 100°C) exploitable for thermal and therapeutic uses, with the intent of creating thermal resorts of tourist interest in the island.

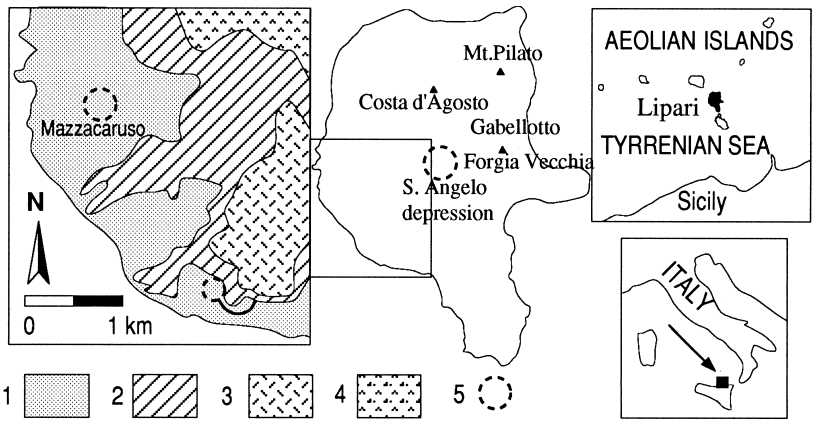

Fig. 1. Geological sketch map of Lipari. (1) basaltic–andesitic lavas (223–150 kyr). (2) Mt. S. Angelo and Costa d'Agosto high-k andesitic lavas and pyroclastics (127–92 kyr). (3) rhyolitic and shoshonitic pyroclastics (42–20 kyr). (4) Gabellotto, Forgia vecchia and Pilato pyroclastics. (5) Crater rims and depressions.

2. Geological settings

The geological formations outcropping in the study area can be divided in three groups on the basis of their permeability: porous rocks (conglomerates, pyroclastic rocks and volcanic soils); fractured rocks (all lava flows of Figs. 2a and 3a) and finally low-permeability rocks (volcanic deposits in lacustrine facies and hydrothermally altered rocks). An ENE tectonic trend in the study area (Principe, 1995) is expressed in the field through a series of faults and fractures almost constantly accompanied by hydrothermal alteration. The presence of hydrothermal activity along such structures constitutes the more convincing proof that these are still active. The alterations permeate large volumes of rock with transformation of primary minerals in mineralogical associations indicating temperatures lower than 200°C (argillitic zone). Further, the presence of wide sulfate (gypsum and anhydrite) mineralizations is characteristic of a sub-surface association of fluids rich in H_2S of probable magmatic origin. High flows of CO_2 have been measured by Chemgeo (1997), both in S. Calogero and Fossa di Fuardo. These values are probably connected with the outgassing of thermal waters relatively rich in CO_2 and relatively close to the earth surface (Chemgeo, 1997).

In both sites of Fossa del Fuardo and Terme di S. Calogero, large alteration zones and hot springs are located near a ENE fault/fracture (Figs. 2 and 3). This led one to assume the presence of a boiling aquiferous in the subsoil and an ascent zone for the geothermal vapor. The northern slope of Fossa del Fuardo is affected by different degrees of hydrothermal alteration. Only in the central area of Fig. 2a it is still possible to recognize a hydrothermally altered cordierite-bearing lava flow that formed by the reaction of metapelite rock with liquid (Barker, 1987). In other parts, the pre-existing lithology has been totally effaced by the alteration and the outcropping rock has taken a typical purplish and/or yellowish-white color. A low-temperature hot spring emerges from these heavily altered rocks near a watershed (Fig. 2a) and is characterized by a flow of less than 2 l/min.

A vast high-argillitic altered area and a thermal sulfate-acid spring (Cimino and Lo Curto, 1996) are also present in Terme di S. Calogero (Fig. 3a). The hot spring has temperatures of the order of 40–50°C and flow of 7–8 l/min (Cimino and Lo Curto, 1996). It is interesting to notice that both Fossa del Fuardo and "Terme di S. Calogero" hot springs are located in close proximity of outcrops of impermeable lacustrine sediments. It is therefore probable that these sediments play an important role for the emergence of thermal water.

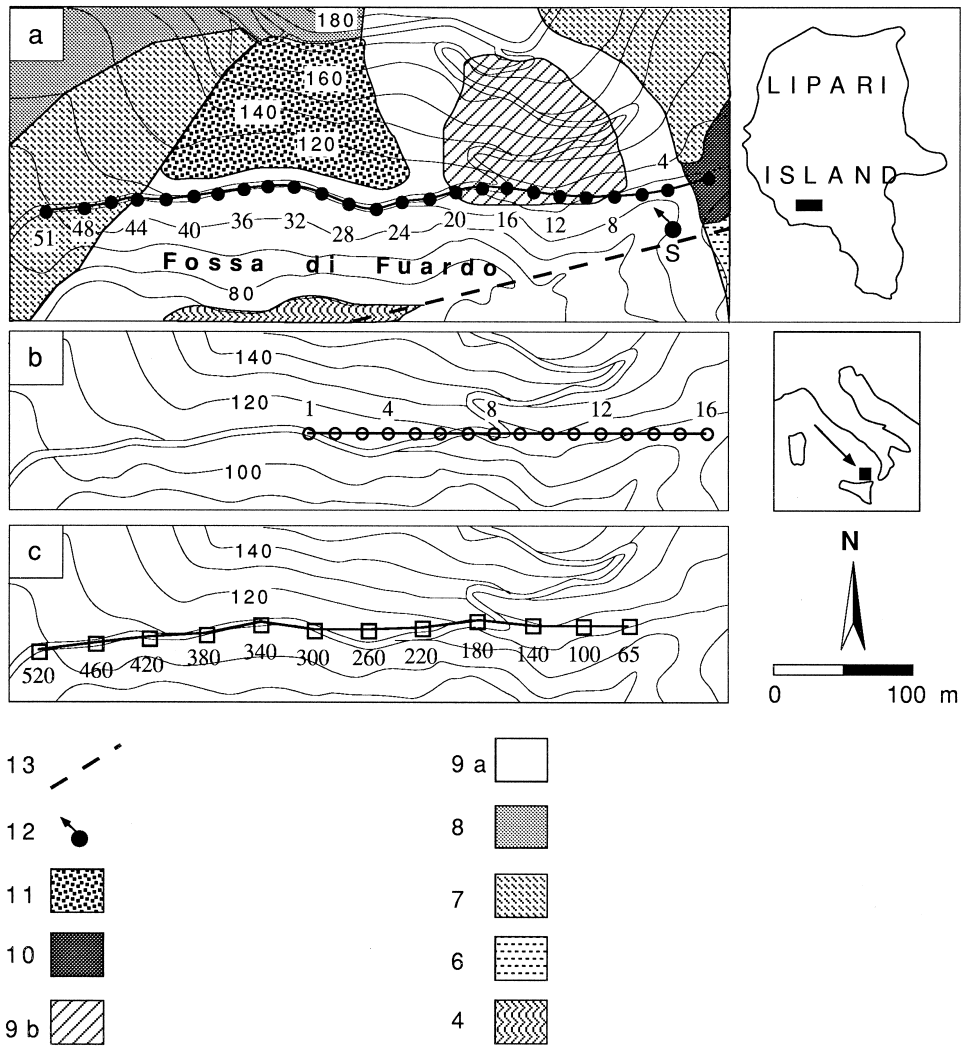

Fig. 2. Geological sketch map (contour interval 10 m) of Fossa di Fuardo: (a) microgravimetric; (b) geoelectric; and (c) seismic surveys. The numbers on microgravimetric and geoelectric surveys show the measurement stations; while those on the seismic survey indicate the distance (in m) from the reference point (station #1 of gravimetric profile). Symbol explanation. (4) Fossa del Fuardo Lava. (6) Lacustrine deposit. (7) Volcanic soil. (8) Cordierite lava. (9a) Loose altered volcanics. (9b) Hydrothermal alteration. (10) Rockslide deposit. (11) Chaotic, partially anthropic debris. (12) Hot spring. (13) Fault. (From Chemgeo, 1997, modified.)

3. Geoelectric survey

3.1. Field operation

The geoelectric survey in Fossa di Fuardo and Terme di S. Calogero (Figs. 2b and 3b), was conducted by using the axial bipole–bipole array technique, which presents a high sensitivity to lateral heterogeneity of resistivity. The bipole technique differs from the dipole arrangement for the fact that the electrode spacing is not negligible with respect to the distance between the bipoles. In each area, a 300-m-long profile was performed with an electrode spacing (a) of 20 m. This spacing allowed a horizontal resolution of 20 m and a theoretical investigation depth of 110 m below the surface. The difference of potential (ΔV) was measured at 10 positions for each bipole source and the apparent resistivity (ρ_a) was

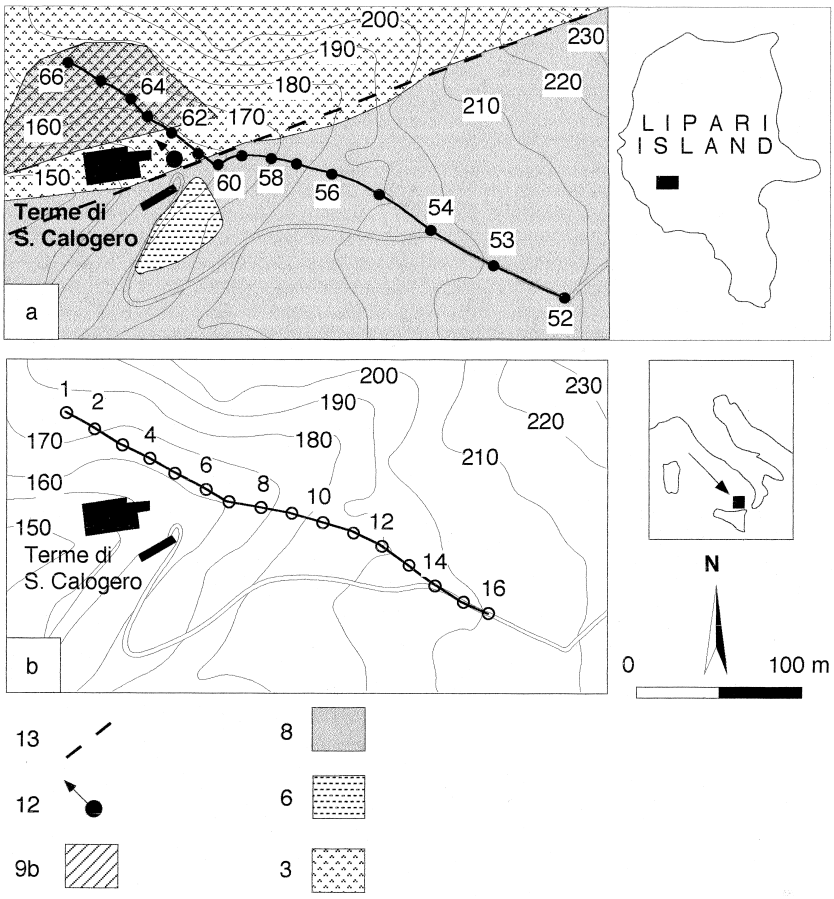

Fig. 3. Geological sketch map (contour interval 10 m) of Terme di S. Calogero. (a) Micogravimetric and (b) Geoelectric surveys. The numbers on the profiles show the measurement stations. Symbol explanation. (3) Mazzacaruso lava. (6) Lacustrine deposit. (8) Cordierite lava. (9b) Hydrotermal alteration. (12) Hot spring. (13) Fault. (From Chemgeo, 1997, modified.)

computed by applying the following formula (Zhdanov and Keller, 1994):

$$\rho_a = \pi na(n+1)(n+2)\Delta V/I \quad (1)$$

where n is an integer which determines the distance between source and measuring bipoles. The motor generator provided us with a 220 V, 50 Hz alternated current: the low frequency used allowed us to apply the mathematical formulas used for direct current (Mauriello, 1997).

3.2. Data interpretation

Interpretation of the results was made on the basis of measured apparent resistivity data and of the geological and volcanological evidences of the area. The pseudo-sections obtained by axial bipole–bipole data acquisition were first interpreted comparing the measured and synthetic apparent resistivity by means of a forward trial and error two-dimensional approach, in order to give a reliable input model to the inversion algorithm. The modeling was carried out using a software based on a Finite Element Method (Rijo, 1977). The preliminary forward models were then tuned up by means of a ridge regression inversion algorithm (Inman, 1975). Data shows a high signal-to-noise (S/N) ratio, therefore no further manipulation (i.e. filtering, etc.) of the geoelectric data set was made.

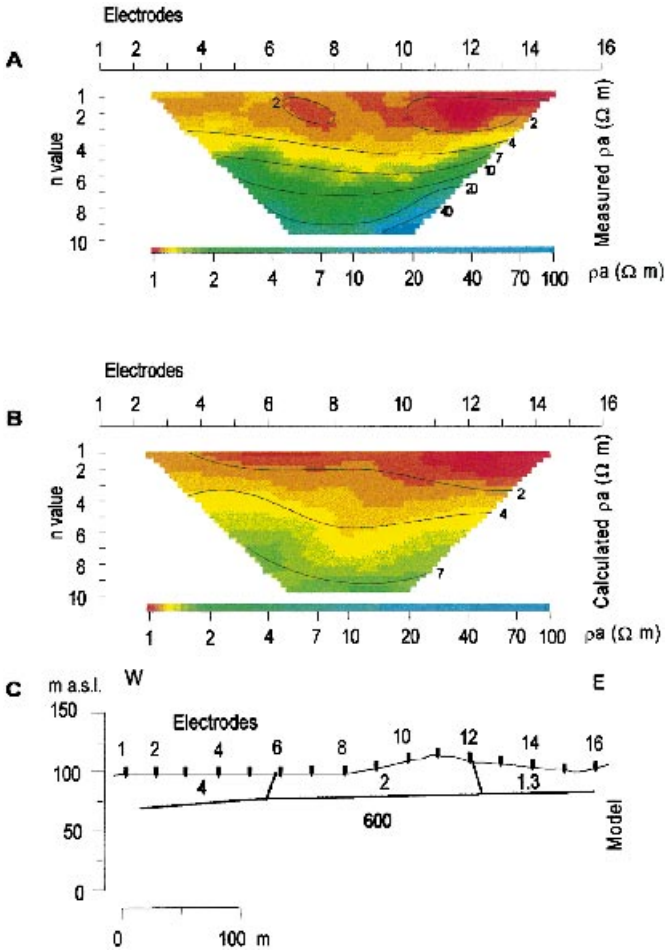

Fig. 4. Measured (A) and calculated (B) pseudo-sections along Fossa di Fuardo. Equal resistivity curves are drawn in black and labeled on the right side of the pseudosections. Measured apparent resistivity increase with depth investigated. Poor agreement between measured and calculated data for *n* greater than 5 is due to a side effect caused by a topographical difference of about 20 m. (C) 2D interpretation of geoelectric profile. Resistivity values are in Ωm. The model is characterized by an upper conductive layer (ρ varying from 1.3 up to 4 Ωm) laying on a lower resistive basement ($\rho = 600$ Ωm).

The measured and synthetic pseudo-sections along Fossa di Fuardo are presented in Fig. 4A and B. Measured data show that ρ_a increases with the depth investigated. The two-dimensional model (Fig. 4C) is then characterized by a 40-m-thick shallow conductive layer, with resistivity varying from 1.3 up to 4 Ωm, overlying on a lower resistive layer ($\rho =$ 600 Ωm). Because of the presence of this shallow conductive layer the actual investigated depth in this site was about 50 m, instead of 110 m.

Comparison of the two pseudo-sections does not show a good agreement between the measured and calculated data for *n* greater than 5 (Fig. 4A and B). This is most probably due to a side effect caused by a topographical difference of about 20 m, whose consequence is the increase of the resistivity on the measured pseudo-section. The presence of this side effect was detected by observing the asymptotic behavior of ρ_a (characterized by a slope greater than 45°) in two soundings extracted from the measured pseudo-section and obtained placing the measuring bipole in positions 12–13 and 15–16.

The measured and synthetic data along Terme di S. Calogero are shown in Fig. 5A and B. In this site the

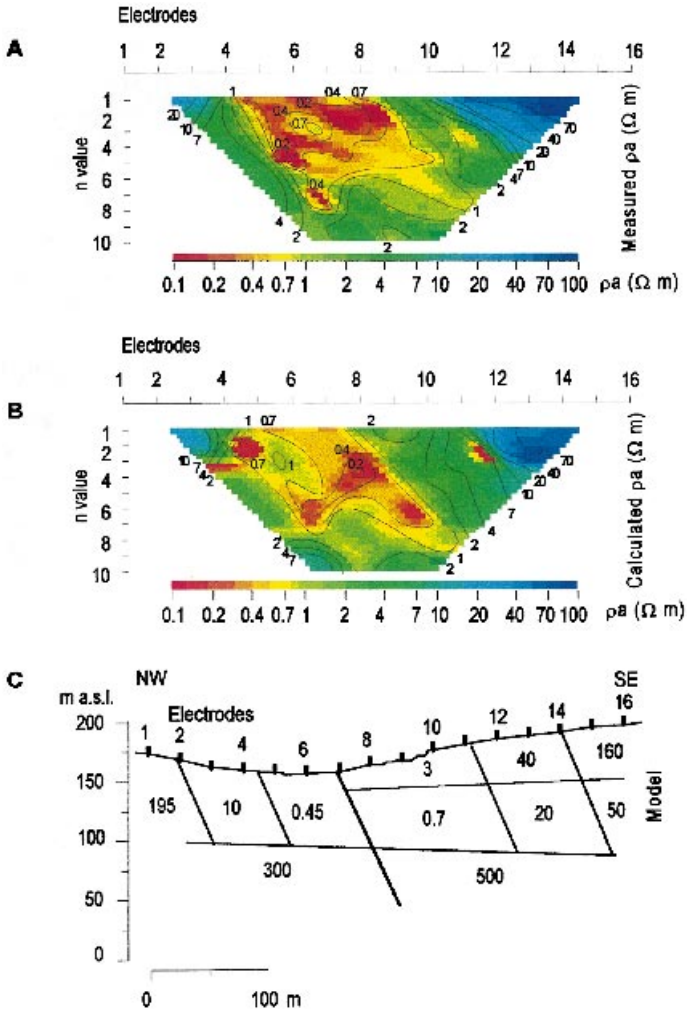

Fig. 5. Measured (A) and calculated (B) pseudo-sections along Terme di S. Calogero. Equal resistivity curves are drawn in black and labeled on the right side of the pseudosections. Measured apparent resistivity (ρ_a) show a central minimum area and two lateral areas with higher ρ_a values. (C) 2D interpretation of geoelectric profile. Resistivity values are in Ωm. The model is characterized by a central zone with very low resistivity values (ρ varying from 0.7 to 10 Ωm) surrounded by higher resistivity zones (ρ varying from 20 to 500 Ωm).

actual investigated depth was about 100 m below the surface. The field data is characterized by low resistivity in the upper middle part of the plot. The two-dimensional model (Fig. 5C) is therefore characterized by a central area with very low resistivity (ρ varying from 0.7 to 10 Ωm), intersected by the ENE trending fault of Fig. 3a and surrounded by higher resistivity media (ρ varying from 20 to 500 Ωm). Comparison between the measured and the calculated pseudosection shows a good correlation.

4. Seismic survey

4.1. Data collection

The seismic reflection profile collected in Fossa di Fuardo (Fig. 2c) is about 400 m long. As a source we utilized the blast of 200 g of explosive set in wells about 2 m deep (Fig. 6). 24 geophone groups, each made of three 14 Hz vertical geophones were used. Such arrays oriented orthogonally to the seismic line, allowed a better soil/receiver coupling and attenuated

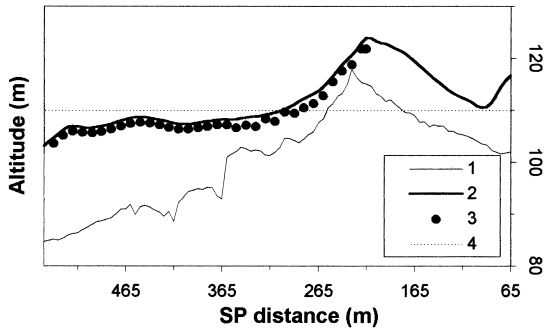

Fig. 6. Topographical and overburden pattern along the seismic profile. Symbol explanation: (1) top of the bedrock; (2) topography; (3) shotpoint positions; (4) datum.

part of the seismic noise generated off-line. The group interval spacing and the source moveout were both set to 5 m. This allowed a maximum Common Depth Point (CDP) fold of 1200% and a spacing of 2.5 m between CDPs. The sampling rate and the record length were set to 500 μs and is 2048 ms, respectively. A "end on" field configuration with a minimum offset ranging between 20–75 m was chosen. Such variable offset simplified the collection procedure as all shotpoints and groups result contiguous. A total number of 864 seismic traces distributed in 154 CDP locations was acquired. The data were pre-processed in the field with a 15 Hz-24 dB/Oct. high-pass filter and A/D converted at 21 bit.

A complex topography and high velocity heterogeneity characterize Fossa di Fuardo. Therefore, in order to proceed to the topographic corrections, six refraction surveys were collected using a portable compact seismic source constituted by a 12″ gauge rifle. Eleven shotpoints and 24 geophone positions were used for each of the six surveys, therefore a total of 1704 traces constitutes the seismic refraction dataset.

4.2. Data processing

The seismic data were processed using the package known as Seismic Unix (SU), developed mainly at the Center for Wave Phenomena (CWP) of the Colorado School of Mines. This shareware package was compiled and installed under Digital UNIX®, version 4.0B on a Digital Alpha server, series 400. Processing

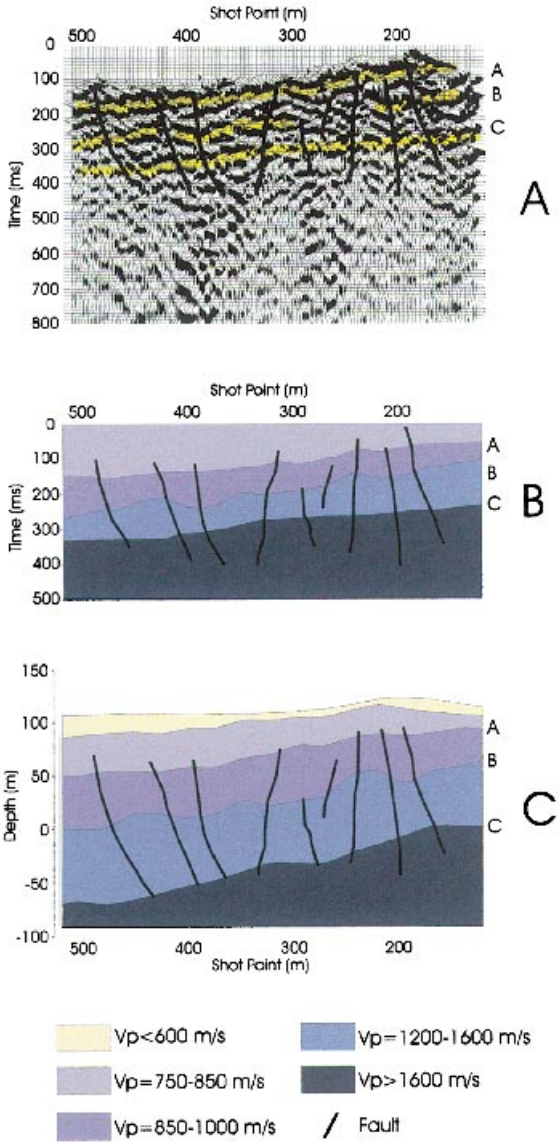

Fig. 7. (A) Zero offset seismic section relative to Fossa del Fuardo survey. (B) Geological and structural interpretation of seismic reflection data. (C) Final seismic reflection and refraction model with times converted in depths referenced to the topographical surface. Refer to the text for the explanation.

the seismic reflection dataset involved considerable time and effort in evaluating pre-processing techniques to enhance the signal. Every shot was examined for noisy traces and high amplitude bursts and many of these noises were manually removed. The final processing flow included spreading correc-

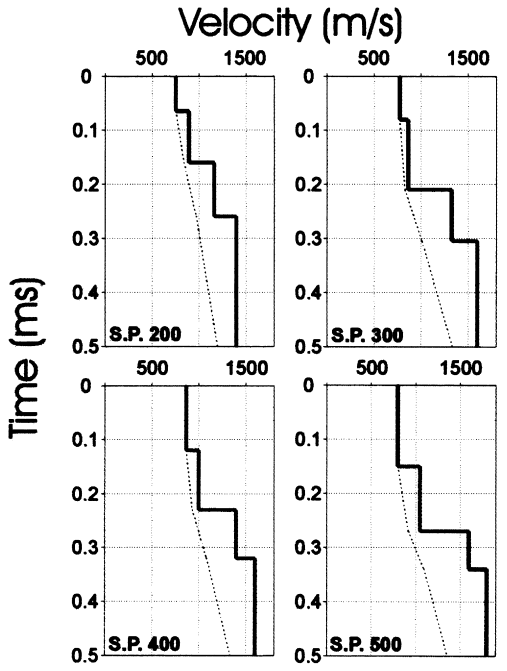

Fig. 8. Interval (continuous line) and stacking (dashed line) P-wave velocity functions calculated along the seismic profile next to shot-point locations 157, 200, 250 and 300. These plots show that a remarkable lateral heterogeneity of seismic velocity, especially within the shallow layers, characterizes the study area.

tions for amplitude balancing, deconvolution and filtering. Noise reduction was crucial. The data were masked by source-generated noise and structure-induced noise. For these data, there were no domains with good separation of signal and noise. The application of band-pass and FK velocity filtering (Ylmaz, 1987; Sheriff and Geldart, 1995) was fundamental, but the noise reduction was not completely effective. The seismic section of Fig. 7 shows in fact strong effects of out-of-plane reflections due to the morphological and structural complexity of the survey area. The near surface of the area showed heterogeneous material properties.

Any coherent wavefield propagating through such a medium will experience differential time delays and will become less coherent. This will affect both signal and noise (Pritchett, 1990). This scattering of signals makes it harder to distinguish signal from noise because both lack coherence. Even in the FK space, the signal and the noise are rarely mutually exclusive. (Beresford-Smith and Rango, 1989).

Since the survey was located over a volcanic area, importance was given to the surface-consistent and residual static corrections. The overburden shape and its velocities were estimated by means of six refraction surveys, interpreted by the Generalized Reciprocal Method ((GRM)-Palmer, 1980). First arrival picking was made using a cross-correlation procedure with MATLAB routines developed for the purpose. High-signal-to-noise (S/N) ratio characterizes the seismic refraction dataset; for this reason there was no need for sophisticated data processing; a 60-Hz low-pass filter (24 dB/Oct.) was only applied before first break picking at large offsets. The height variations along the seismic reflection profile were instead estimated by means of an accurate topographic leveling made every 10 m during the gravity survey. The estimated error on such measures is of the order of 1 cm. In Fig. 6 are the overburden and the topography shape estimated by the seismic refraction and the topographic leveling. The datum level was positioned at a height of 110 m above sea level (a.s.1.).

Great importance was given to velocity analysis. High lateral velocity variations on Fossa del Fuardo rendered this part difficult. To account for nonhyperbolic moveout, the exact expression for the azimuth-dependent quartic term of the Taylor series traveltime expansion, derived by Tsvankin and Thomsen (1994), was utilized for normal moveout (NMO) correction. Stacking, velocity analysis and residual static corrections were applied iteratively. Residual static corrections were estimated by maximizing the stack power in a window that included the main reflections (25–400 ms). The data were not migrated, in part because migration of shallow reflectors often is not needed (Black et al., 1994) and in part to avoid further degradation of data quality (due to a large indetermination on the velocity analysis, especially for the deeper reflectors).

4.3. Data interpretation

On the zero offset section drawn in Fig. 7A, three main reflectors are visible: the uppermost reflector (A) has arrival times included between 50–160 ms, Two Way Time (TWT), and onlaps a second reflector (B) with arrival times between 150–300 ms, which seems to be more discontinuous and irregular. A third

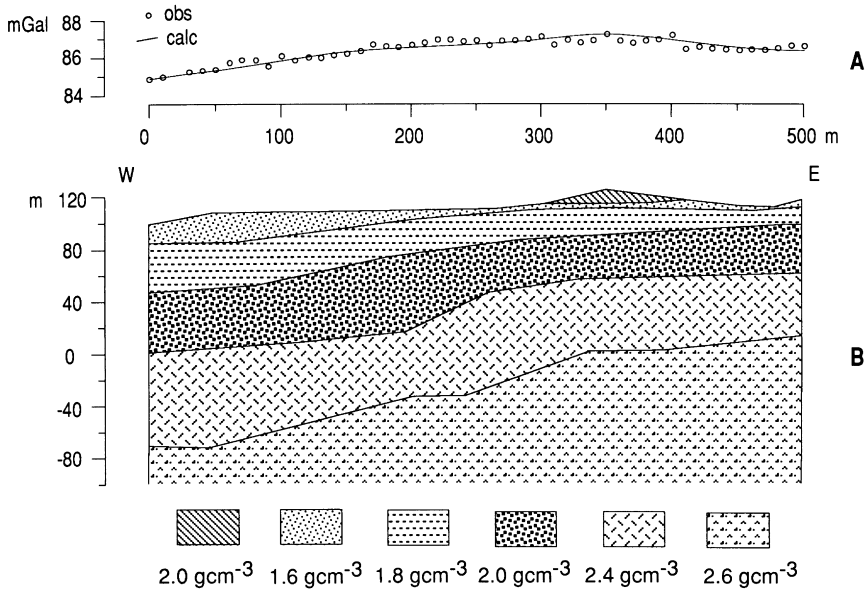

Fig. 9. (A) Bouguer anomaly along Fossa di Fuardo. The solid line shows the calculated data. (B) Gravimetric model along Fossa di Fuardo. The numbers on labels indicate the δ values in g/cm^3.

reflector (C) with a more regular trend is found at 260 ms TWT on the right end of the section. Since other continuous reflectors are hardly identifiable below reflector C, this will be considered in this work as the seismic basement. The reflecting horizons are interrupted by numerous sub-vertical discontinuities. These last can be explained as fractures or faults with throw values that are of the order of vertical resolution of the seismic method.

The final model with times converted in depths referenced to the topographical surface is shown in Fig. 7C. The model also includes the morphology of the overburden layer, detected by seismic refraction data. Depths of reflectors A, B and C were estimated using the surface interval velocity functions calculated by means of the Dix (1955) formula. In general, depths calculated by the surface velocity functions are affected by a 10% average error (Sheriff and Geldart, 1995). However, in our case, no well allowed a direct checking of the quality of our depth determinations and therefore of the quality of velocity analysis. Therefore, we cannot be sure that the error on velocity is within the limit of 10%. For safety reasons, since we are dealing with volcanic lithotypes, a greater error, increasing with the depth (10, 15 and 20% on reflectors A, B and C) should be accounted on our depth determinations. All seismic discontinuities show a slight dip toward the sea (to the W on the section of Fig. 7C) that increases with the depth (about 6° for reflector A and 11° for reflector C). This trend is similar to that of the other volcanic layers present in the area. Except for some local conditions there is a general increase of seismic velocity with the depth (see Fig. 8). This increment is very pronounced at the third discontinuity of Fig. 7, located at about the seal level to the W of the section. Few hundred meters to the S of the survey, near the seashore there is a contact between the bottom of a thick pyroclastic layer and the top of the basaltic–andesitic lavas (see Fig. 1). It is therefore probable that the sharp velocity increment at the interface B corresponds to this lithological change.

5. Microgravimetric survey

5.1. Data acquisition

The microgravimetric survey was carried out along two profiles in Fossa di Fuardo and Terme di S.

Calogero (Figs. 2a and 3a). The profile collected in Fossa di Fuardo is 500 m long and is made of 50 measure points (from #1 up to #51), placed every 10 m. At point #3 the measure was not performed because of the very difficult logistic of this site. The profile carried out in Terme di S. Calogero is about 400 m long and counts 15 measuring points (from #52 up to #66), placed at about every 25 m, depending on the logistic of the area.

Gravity data were collected using the La Coste & Romberg microgravimeter (mod. D-137), with sensitivity of ± 5 μgal. The reference station of the surveys was placed in the Marina Corta site, which is part of the Aeolian gravimetric network set up by the Osservatorio Vesuviano for geophysical surveillance; the gravity value in this station is 980134.719 mgal (Berrino, personal communication).

The height of stations was obtained by a precise topographic survey. The error on measure is less than 1 cm. The gravity data were corrected for lunar–solar tide and instrumental drift and were then processed for routine corrections. Bouguer and terrain corrections were performed assuming a density of 2.2 g/cm^3 for Fossa di Fuardo and of 2.5 g/cm^3 for Terme di S. Calogero. These values were obtained considering the geology of the area and the lithology of the outcrops present along the profiles. The terrain correction was computed spherically up to a distance of 6653 m of each station (J zone) following the scheme of Hammer (1939). Corrections were referred, for each profile, to the surface having the point with lowest altitude, i.e. station #51 (height of 100.855 m a.s.l.) for Fossa di Fuardo profile and station #61 (height of 157.369 m a.s.l.) for Terme di S. Calogero profile. Gravity values were computed using the International formula of the Geodetic Reference System 1980 (Moritz, 1984). Bouguer anomalies obtained for the two profiles are shown in Figs. 8 and 9.

5.2. Data interpretation

The interpretation was carried out using a forward trial-and-error method. The gravity model resulted by comparison of the gravity field, computed by a 2.75D finite element code, with the observed gravity. Based on geological considerations, the body dimensions were extended for 100 m in the direction orthogonal to the profiles. In any case, because of the poor lateral continuity of the shallow volcanic rocks, their effect on gravity was kept in due count. To simplify the interpretation, the results of the seismic survey were used as constraints in order to define the geometry of some interfaces between layers with different densities.

The general trend of the Bouguer anomaly in Fossa di Fuardo shows an increase from a value of 85 mgal at the western extreme of the profile up to a maximum of 87 mgal in the central part, and then a slight decrease down to a value of 86 mgal (Fig. 9A). On the geological map (Fig. 2a) two geological formations outcrops in the survey area: (a) loose volcanic rocks, too altered that the original lithology is unrecognizable; and (b) a little strip of altered cordierite lava. The gravity model reported in Fig. 9B exhibits as first layer an altered volcanic deposit with density of 1.6 g/cm^3. The outcropping altered cordierite lava lens was crossed in the E side of the profile (see Fig. 2a). A density of 2.0 g/cm^3 was assigned to such a body. The second and the third layer, both about 40 m thick and roughly dipping toward the W, were modeled assigning a density of 1.8 and 2 g/cm^3, respectively. The fourth layer and the basement are characterized instead by higher density values (2.4 and 2.6 g/cm^3, respectively), typical of lava beds.

The second profile crosses the thermal rising of S. Calogero and cuts with a right angle the gorge and the fault marked on the geological map (Pichler, 1976). Such a profile is virtually coincident with one of the two geo-electric profiles. Signals show a step shaped anomaly (Fig. 10A), typical of a fault that put in contact two rocks with different density values. Fig. 10B shows the geophysical model, built also based on the geological outcrops of the area (Fig. 3a). Two lava formations outcrop along the profile: a lava flow originated from Mt. Mazzacaruso (see Fig. 1; left inset) on the western side of the profile and the cordierite lava bank on the eastern side. Identical densities (2.5 g/cm^3) were assigned to both lava banks. The density contrast along the fault is due to the presence on its downthrow (E) side, of an about 80 m thick bank of lacustrine sediments with an assigned density of 1.5 g/cm^3, below the cordierite lava. Besides, such sediments outcrop for approximately 10 m to the S of the survey area.

The anomaly calculated with this model reproduces the experimental filtered data within an acceptable

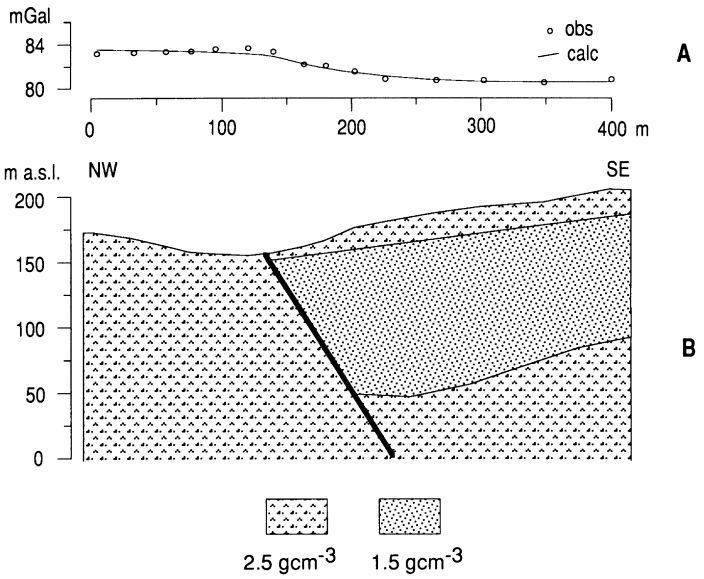

Fig. 10. (A) Bouguer anomaly along terme di S. Calogero. Solid line shows the calculated data (B) Gravimetric model along Terme di S. Calogero. The numbers on labels indicate the δ values in g/cm^3.

error margin. The greater errors are at a distance of 120–140 m, where the data are compatible with the presence of a shallow high-density body even if with a narrow horizontal extension.

6. Conclusions and discussion

It is well known that, without a specific geological setting resulting from exploration wells, each geophysical method often allows only a semi-quantitative investigation of subsurface structures, especially if we deal with the very complex morphology and structure of a volcanic island. On the contrary, an exploration strategy of geothermal resources based on geophysical methods, which are less expensive than exploratory wells, is convenient since the risk of a subsequent vain exploration by wells can be drastically reduced. In our survey, a satisfying outcome in underground investigation was obtained by a continuous comparison of results of different geophysical methods, since each method investigated for different physical parameters and consequently, made possible the definition of some geological constraints. Integration of the results obtained by each method in the investigated sites allowed us to make some important considerations about the shallow low enthalpy resources in the SW sector of the island. Evaluation of the actual potential of these resources, utilized since ancient times, could bring to their future appropriate exploration for tourist and health aims and therefore might represent an important heading of the local economy of the island.

In our survey we collected four data sets for Fossa di Fuardo (microgravimetric, geoelectric and seismic reflection and seismic refraction surveys) and two data sets for Terme di S. Calogero (microgravimetric and geoelectric surveys). The final interpretation for the two investigated areas, carried out by joining and integrating the different results and constrains obtained by each methodology, is presented here and is condensed in Fig. 11.

Fossa di fuardo. Due to logistic problems, in Fossa del Fuardo the survey did not intersect the fault and the hot spring of the area, since they are placed in an uneven area difficult to access. The geophysical surveys were carried out along a mule-track that crosses the hydrothermal altered zone (Fig. 2a). This site is characterized by the highest flux of CO_2 in the island. The shape of the areas characterized by high CO_2 fluxes suggests that thermal hot water infiltrates the

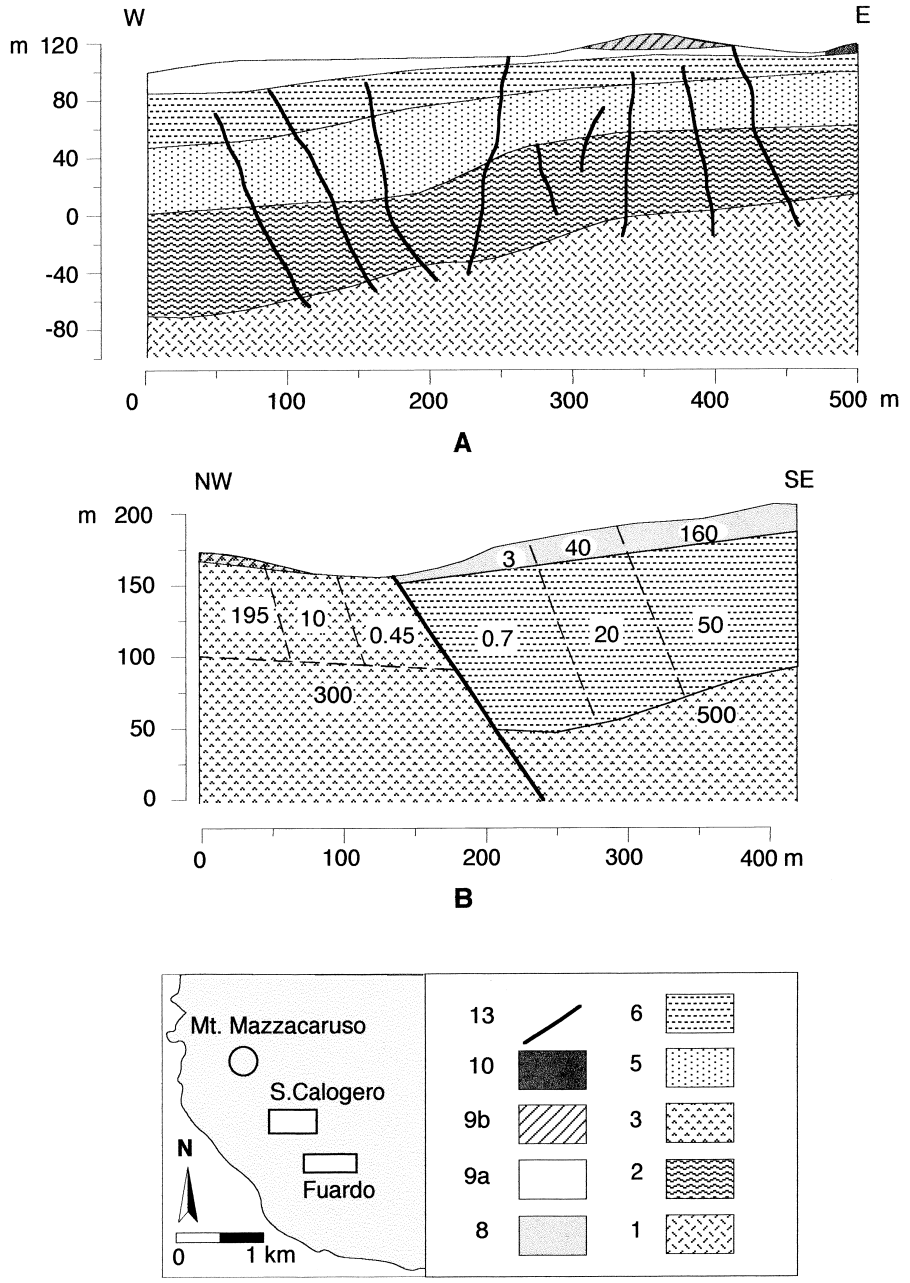

Fig. 11. (A) Integrated geophysical (gravimetric, geoelectric and seismic) and geological model of Fossa di Fuardo. Symbol explanation. (1) Submarine lavag ($V_p = 2000$ m/s, $\delta = 2.6$ g/cm^3). (2) Ancient Basalt-Andesitic Lava ($V_p = 1500$ m/s, $\delta = 2.4$ g/cm^3). (5) Pyroclastic deposit ($V_p = 800-900$ m/s, $\delta = 2.0$ g/cm^3, $\rho = 600$ Ωm). (6) Lacustrine deposit ($V_p = 800$–900 m/s, $\delta = 1.8$ g/cm^3, $\rho = 1.3-4$ Ωm). (8) Cordierite lava ($V_p < 600$ m/s, $\delta = 2.0$ g/cm^3, $\rho = 1.3-4$ Ωm). (9a) Loose altered volcanics ($V_p < 600$ m/s, $\delta = 1.6$ g/cm^3, $\rho = 1.3-4$ Ωm). (9b) Hydrothermal alteration. (10) Rockslide deposit. (13) Fault. (B) Integrated geophysical (gravimetric and geoelectric) and geological model of Terme di S. Calogero. Symbol explanation. (3) Mazzacaruso lava ($\delta = 2.5$ g/cm^3, $\rho = 0.45$–500 Ωm). (6) Lacustrine Deposit ($\delta = 1.5$ g/cm^3, $\rho = 0.7$–50 Ωm). (8) Cordierite lava ($\delta = 2.5$ g/cm^3, $\rho = 3$–160 Ωm). (13) Fault. Resistivity values plotted in the figure are in Ωm.

shallow aquiferous and mixes with cold (poor in CO_2) groundwater spreading out laterally (Chemgeo, 1997).

Interpretation of the seismic refraction and seismic reflection dataset allowed us to locate four subsurface discontinuities roughly dipping toward the sea (Fig. 7c). The seismic model is compatible with models obtained by microgravimetric (Fig. 9) and electric (Fig. 4c) surveys, although the depth penetration of the electric profile is confined to reflector "B", due to the presence of a shallow conductive layer.

The first discontinuity was detected by seismic refraction and should correspond to the lower limit of the hydrothermally altered outcrop. The fact that this upper layer is characterized by low seismic wave velocity ($V_p < 600$ m/s), very low resistivity ($\rho < 5\ \Omega$m) and a density of 1.6 g/cm^3 strengthen our interpretation. The thickness of this layer was evaluated in about 15–20 m on the W side of the profile.

The second layer is characterized by an average P-wave velocity of about 800 m/s, a density of 1.8 g/cm^3 and by low resistivity ($\rho < 5\ \Omega$m). These geophysical parameters are compatible with clay deposits. This hypothesis is confirmed by geological evidence, which shows the presence of volcanic deposits in lacustrine facies to the SE of the profile (lithotype 6 in Fig. 2a).

The third layer, about 40 m thick, is characterized by P-wave velocities and densities not much different from those of the second layer ($V_p \approx 900$ m/s and $\delta = 2.0$ g/cm^3) but by remarkably higher resistivity (about 600 Ωm). This high resistivity can only be attributed to the upper portion of such layer, which corresponds with the actual depth investigated by the geoelectric survey (about 50 m below the surface). Based on these results and of geological information, it is probable that pyroclastic deposits, which appear to be dry at least in their upper portion, compose this layer. For completeness of information it should also be noticed that the horizontal resolution of resistivity data is about 20 m. It is therefore possible that localized low resistivity areas such as sub-vertical fluid-filled fault and/or fracture zones are not detected by the geoelectric survey. The bottom of this pyroclastic formation outcrops at the sea level at a distance, from the survey, of about 400 m to the SW (Chemgeo, 1997).

The limit between the third and the fourth layer is characterized by an abrupt increase in the average P-wave velocity and density ($V_p \approx 1400$ m/s; $\delta = 2.4$ g/cm^3) and may therefore be interpreted as the top of the old basalt-andesitic lavas. These lavas outcrop near the seashore at a distance, from the investigated site, of about 400 m to the SW (Pichler, 1976; Chemgeo, 1997). The thickness of these lava flows was evaluated to be about 60 m.

Finally, higher P-wave velocities and density of 2.6 g/cm^3 characterize the basement that may be composed of basalt-andesitic lavas erupted in a submarine environment. This interpretation is only supported by the geophysical data, which detected the top of the formation below sea level (see Fig. 11A).

Seismic data also showed the presence of some subvertical fractures along the survey (Fig. 7), not clearly visible at the surface because of the impressive hydrothermal alteration which characterizes the area. The presence of some of these fractures at the surface is also confirmed by the geoelectric survey (Fig. 4C), which detected two lateral resistivity changes inside the upper conductive layer ($\rho < 5\ \Omega$m). The first one is located below electrode #7 and coincides with the fracture detected by the seismic survey at the shot-point (SP) location #190 in Fig. 7; the other one is found below electrode #13, next to the ENE trending fault and to the hot spring (Fig. 2a). It is very likely that these fractures had an important role in the past in conveying the thermal water up to the surface. At present, only a hot spring with very low flow rate is visible near the ENE trending fault (Fig. 2a). This may be due to the hydrothermal alteration with formation of clay minerals, which can cause the obstruction of the faults/fractures and the migration of the emergence with time.

On the basis of the geophysical model described above (Fig. 11), it may be argued that the first two layers (altered deposits and lacustrine deposits), both characterized by very low permeability, could act as a boundary and force the geothermal fluids to upraise only along the few not-obstructed fractures. Therefore, in order to extract thermal fluids, it could be convenient to bore through the shallow impermeable formations down to the bottom of the underlying pyroclastic deposits and fractured lava banks (lithotype 5 in Fig. 11A) which could represent the low-enthalpy geothermal reservoir of the area. The highest probability of locating thermal fluids, especially into

the lava banks, is obviously found in correspondence of the ENE fault and the detected fractures which seem to interest all the bodies including the basement (see Fig. 11A).

Terme di S. Calogero. At Terme di S. Calogero microgravity and geoelectric surveys were carried out along a morphologic low which, according to geologic evidences, was due to a fault (Fig. 3a). Very close to this fault, there is an important hot spring. The waters have a sodium bicarbonate–sulfate composition and neutral pH (Cimino and Lo Curto, 1996). The spring water temperature decreased from more than 90°C, in 1872, to 60°C, in the period 1906–1972, to 47°C, at present (Cimino and Lo Curto, 1996). During a preliminary survey made by Chemgeo (1997) it was supposed that the thermal spring is fed by shallow meteoric waters warmed by geothermal vapors rich in acid gasses (CO_2 e H_2S).

Results obtained by the two geophysical surveys show a good agreement. The gravity survey clearly exhibits, in the central part of the investigated area, the presence of the ENE fault which, in the south-eastern side of the profile, displaces downwards of approximately 100 m a body with a density of 2.5 g/cm^3. This formation was interpreted as a lava flow originated from Mt. Mazzacaruso (lithotype 3 in Fig. 3a). An approximately 100 m thick layer with a density of 1.5 g/cm^3 and interpreted as a lacustrine deposit (lithotype 6 in Fig. 3a) overlies the Mazzacaruso lava in the downthrow side. Finally the outcropping formation is a 10–20 m thick, cordierite-bearing lava flow with density of 2.5 g/cm^3 (lithotype 8 in Fig. 3a).

Geoelectric interpretation shows, on both W and E sides of the fault, an area, about 60–80 m thick and approximately 150 m wide, with very low resistivity (ρ varying from 0.7 up to 10 Ωm, according to the saturation degree and temperature) that is probably characterized by geothermal circulation. This area is centered on the fault plane and has partial evidence at the surface (i.e. the hydrothermally altered zone shown in Fig. 3a). Deeper rocks are characterized by quite higher resistivity (300–500 Ωm), even in close proximity of the fault plane. It follows that no electric evidence of geothermal fluids uprising along such faults is visible from the data. On the contrary, as already discussed, the horizontal resolution of geoelectric data in both sites is of about 20 m; consequently, if the width of the ascent zone is less than 20 m, the latter is not detected by our survey. Therefore it cannot be excluded that deep geothermal fluids upraise along the fault surface which could be less than 20 m wide within the deep compact rocks. Where the fault surface intersects the shallower formations, the fault zone widens, and the hot fluids may spread out laterally and mix with the cold shallow infiltration waters. This mechanism explains the shape of the areas characterized by high CO_2 fluxes in the site (Chemgeo, 1997).

Based on our data, it cannot be asserted that the above-mentioned mechanism occurs exactly in the investigated area. The ascent zone may also be located morphologically above the spring area, probably still along the fault surface. The hot fluids then mix with the sallow waters, flow downstream within the subsurface layers intersected by the fault zone and finally emerge in correspondence of Terme di S. Calogero probably because of morphological reasons and/or the contact of the impermeable sediments on the right side of the fault. In order to locate the exact point where the raising of deep fluids may occur it could be convenient to plan further high-resolution geochemical and geophysical surveys along the ENE trending fault site.

Acknowledgements

We wish to thank the authorities of the Township of Lipari for their willingness and kindness; in particular Domenico Russo, geologist, for his qualified and enthusiastic participation in the field work. A special thanks to Eugenio Carrara for his helpful suggestions in the field and during the reviewing of this manuscript; Vincenzo Di Fiore for the precious help given during the acquisition phase of the seismic data, for his competent processing of the seismic refraction data and for important assistance in seismic reflection processing; Vincenzo D'Isanto, indispensable in the field; Giovanni Florio who conducted the preliminary inspection of the sites and part of the gravity data processing and interpretation; Gaetano Paolillo for his precious help given at various stages of the gravity survey. We also thank Sami Jazairi of the University of Utah for careful reviewing of the manuscript.

References

Alvarez, W., 1976. A former continuation of the Alps. Geol. Soc. Am. Bull. 87, 891–896.

Alvarez, W., Cocozza, T., Wezel, F.C., 1974. Fragmentation of the Alpine orogenic belt by microplate dispersal. Nature 248, 309–314.

Anderson, H., Jackson, J., 1987. The deep seismicity of Tyrrhenian sea. Geophys. J. R. Astron. Soc. 91, 937–983.

Barberi, F., Gandino, A., Gioncada, A., La Torre, P., Sbrana, A., Zenucchini, C., 1994. The deep structure of the Eolian arc (Filicudi–Panarea–Vulcano sector) in light of gravity, magnetic and volcanological data. J. Volcanol. Geotherm. Res. 61, 189–206.

Barker, D.S., 1987. Rhyolite-contaminated with metapelite and gabbro, Lipari, Italy, products of lower crustal fusion or assimilation plus fractional cristallization?. Contrib. Mineral. Petrol. 97, 460–471.

Beresford-Smith, G., Rango, R., 1989. Suppression of ground roll by windowing in two domains. First Break 7, 55–63.

Biji-Duval, B., Letouzey, J., Montadert, L., 1987. Structure and evolution of the Mediterranean basins. Initial Rep. Deep Sea Drill Proj. 42 (1), 951–984.

Black, R., Steeples, D.W., Miller, D., 1994. Migration of shallow seismic reflection data. Geophysics 59, 402–410.

Chemgeo, 1997. Progetto di valorizzazione delle risorse termali dell'area dei Bagni di S. Calogero. Unpublished paper, Comune di Lipari, prot. N. 41081, 11/11/1997.

Cimino, G., Lo Curto, R., 1996. Le acque termali di S. Calogero a Lipari (ME) ì. Accertamenti chimici, chimico-fisici e microbiologici. Rapporto del Dip. di Chimica Org. e Biol. Univ. Of Messina, 14pp.

Cortese, G., Frazzetta, G., La Volpe, L., 1986. Volcanic history of Lipari (Aeolian Islands Italy) during the last 10,000 years. J. Volcanol. Geotherm. Res. 27, 117–183.

Crisci, G.M., De Rosa, R., Lanzafame, G., Mazzuoli, R., Sheridan, M.F., Zuffa, G., 1991. Monte Guardia sequence: a late Pleistocene eruptive cycle on Lipari Italy. Bull. Volcanol. 44, 241–255.

De Rosa, R., Sheridan, M.F., 1983. Evidence for magma mixing in the surge deposits of the M.te Guardia sequence (Lipari). J. Volcanol. Geotherm. Res. 17, 313–328.

Dix, C.H., 1955. Seismic velocities from surface measurements. In: Byun, S. (Ed.), Velocity Analysis on Multichannel Seismic Data. Geophysics, 20, pp. 68–86.

Esperanca, S., Crisci, G.M., De Rosa, R., Mazzuoli, R., 1992. The role of the crust in the magmatic evolution of the island of Lipari. Contrib. Mineral. Petrol. 112, 450–462.

Frazzetta, G., Lanzafame, G., Villari, L., 1982. Deformazioni e tettonica attiva a Lipari e Vulcano (Eolie). Mem. Soc. Geol. It. 24, 294–297.

Gillot, P.Y., 1987. Histoire volcanique des Iles Eoliennes: arc insulaire or complexe orogenique anulaire?. D.T. IGAL 11, 35–42.

Hammer, S., 1939. Terrain corrections for gravimeter stations. Geophysics 4, 184–194.

Inman, J.R., 1975. Resistivity inversion with ridge regression. Geophysics 40 (5), 798–817.

Keller, J., 1970. Die historischen Eruptionen von Vulcano und Lipari. Z. Dtsch. Geol. Ges. 121, 23–58.

Lanzafame, G., Bousquet, J.C., 1997. The Maltese escarpment and its extension from Mt. Etna to Aeolian Islands (Sicily): importance and evolution of a lithospheric discontinuity. Acta Vulcanol. 9, 121–135.

Locardi, E., Nappi, G., 1979. Tettonica e vulcanismo recente nell'isola di Lipari (implicazioni geodinamiche). Boll. Soc. Geol. It. 98, 447–456.

Mauriello, P., 1997. Tomografia Elettromagnetica. PhD thesis. Università degli Studi di Napoli Federico II. Bibl. Naz. Firenze and Roma.

Moritz, H., 1984. Geodetic reference system 1980. In: Tscherning, C.C. (Ed.). The Geodesist's Handbook, Bull. Geod., 58, pp. 388–398.

Palmer, D., 1980. The generalized reciprocal method of seismic refraction interpretation. SEG, Tulsa OK.

Pichler, H, 1976. Carta geologica dell'Isola di Lipari (scala 1:10,000). Firenze-litografia artistica cartografica.

Pichler, H., 1980. The island of Lipari. Rend. Soc. It. Miner. Petr. 36, 415–440.

Principe, C., 1995. Studio vulcanotettonico preliminare dell'Isola di Lipari. J.V. Agip-Enel-Ems, AGIP, Esplorazione geotermica.

Pritchett, W.C., 1990. Acquiring better seismic data. Chapman and Hall, London.

Rijo, L., 1977. Modeling of electric and electromagnetic data. PhD thesis, University of Utah, University Microfilms International, Ann Arbor, Michigan.

Sheriff, R.E., Geldart, L.P., 1995. Exploration Seismology, 2nd ed. Cambridge University Press, Cambridge, 419 pp.

Tortorici, L., Ventura, G., Mazzuoli, R., Monaco, C., 1995. Stutture del settore orientale dell'Arcipelago Eoliano: interpretazione tettonica e modelli numerici. Studi Geologici Camerti 2, 455–466.

Tsvankin, I., Thomsen, L., 1994. Nonhyperbolic reflection moveout in anysotropic media. Geophysics 59, 1290–1304.

Ventura, G., 1994. Tectonics, structural evolution and caldera formation on Vulcano Island (Aeolian Archipelago, Southern Tyrrhenian Sea). J. Volcanol. Geotherm. Res. 60, 207–224.

Ventura, G., 1995. Relazioni fra tettonica e vulcanismo nel settore orientale delle Eolie (Salina, Lipari, Vulcano, Panarea, Stromboli). Proc. 14th Nat. Conv. GNGTS-CNR, pp. 957–965.

Ylmaz, O., 1987. Seismic data processing. In: Doherty, S.M. (Ed.). Soc. Explor. Geoph., Investigation in Geophysics, 2. , p. 526.

Zhdanov, M.S., Keller, G.V., 1994. The geoelectrical methods in geophysical exploration. Elsevier, Amsterdam, 873 pp.